JOURNAL OF GEOPHYSICAL RESEARCH, VOL. 113, D18203, doi:10.1029/2008JD009791, 2008

Effect of clouds on the calculated vertical distribution of shortwave absorption in the tropics

Sally A. McFarlane,[1] James H. Mather,[1] Thomas P. Ackerman,[2] and Zheng Liu[3]

Received 5 December 2007; revised 29 May 2008; accepted 26 June 2008; published 23 September 2008.

[1] High vertical resolution profiles of cloud properties were obtained from cloud radars operated by the Atmospheric Radiation Measurement (ARM) program on the islands of Nauru and Manus in the Tropical Western Pacific (TWP). Broadband flux calculations using a correlated *k*-distribution model were performed to estimate the effect of clouds on the total column and vertical distribution of shortwave absorption at these tropical sites. Sensitivity studies were performed to examine the role of precipitable water vapor, cloud vertical location, optical depth, and particle size on the shortwave (SW) column absorption. On average, observed clouds had little impact on the calculated total SW column absorption at the two sites, but a significant impact on the vertical distribution of SW absorption. Differences in the column amount, vertical profiles, and diurnal cycle of SW absorption at the two sites were due primarily to differences in cirrus cloud frequency.

Citation: McFarlane, S. A., J. H. Mather, T. P. Ackerman, and Z. Liu (2008), Effect of clouds on the calculated vertical distribution of shortwave absorption in the tropics, *J. Geophys. Res.*, *113*, D18203, doi:10.1029/2008JD009791.

1. Introduction

[2] Radiative heating by clouds is an important component of the total diabatic heating of the atmosphere [*Johnson and Ciesielski*, 2000]. Although the radiative effects of clouds on the Earth's energy budget are most readily seen by examining top-of-atmosphere (TOA) and surface fluxes, their direct effect on the atmospheric circulation is through the redistribution of energy vertically in the atmosphere, which has important impacts on local and large-scale atmospheric dynamics and the hydrological cycle [*Stephens*, 2005]. *Wang and Rossow* [1998] illustrate that changing the vertical structure of clouds in a General Circulation Model (GCM), while retaining the total cloud cover, water path, and particle size, affects the large-scale Hadley circulation directly by modifying the radiative cooling profile and atmospheric stability and indirectly by affecting the latent heating profiles. Although measurements of top-of-atmosphere and surface fluxes enable calculation of the total amount of absorption in the column, understanding how clouds act to redistribute energy within the atmospheric column requires measurements of clouds at high vertical resolution. The cloud and radiation measurement sites developed by the Department of Energy's Atmospheric Radiation Measurement (ARM) program in the Tropical Western Pacific (TWP) provide long time series of remote sensing measurements of cloud properties, from which we calculate estimates of the vertical distribution of solar absorption in the atmosphere with corresponding high resolution.

[3] Examination of column shortwave (SW) absorption in cloudy atmospheres has a long history [see discussion in *Stephens and Tsay*, 1990; *Ackerman et al.*, 2003]. Several studies in the mid-1990s [*Cess et al.*, 1995; *Arking*, 1996] that compared observations of SW column absorption (obtained from combining surface and satellite radiation measurements which had very different horizontal resolutions) to radiative transfer model results found that the models consistently underestimated the amount of absorption in the atmospheric column by significant amounts (up to 30%). Many explanations were put forth as possible solutions to this discrepancy including sampling uncertainties, observational errors, aerosol, and missing physics in radiative transfer models. Theoretical studies of clear-sky absorption with very detailed spectral radiative transfer models [*Crisp*, 1997] and observational studies [*Solomon et al.*, 1998] found little evidence for missing absorbers that could explain differences of such magnitude. Additional studies investigated the spectral characteristics and theoretical limits of cloudy sky absorption, using modeled or idealized clouds [*Ramaswamy and Freidenreich*, 1998; *Crisp*, 1997; *Lubin et al.*, 1996]. More recent observational studies, in which layer absorption was calculated by combining surface measurements with aircraft measurements of fluxes directly above overcast clouds, largely disproved the possibility of dramatically enhanced SW absorption by clouds [*Ackerman et al.*, 2003; *Asano et al.*, 2000; *O'Hirok and Gautier*, 2003]. These studies found smaller disagreements (on the order of 10 W m^{-2}) when compared to calculations from radiative transfer models with updated gas absorption treatments, although some studies still indicate a

[1]Climate Physics Group, Pacific Northwest National Laboratory, Richland, Washington, USA.
[2]Joint Institute for the Study of the Atmosphere and Ocean and Department of Atmospheric Sciences, University of Washington, Seattle, Washington, USA.
[3]Department of Atmospheric Sciences, University of Washington, Seattle, Washington, USA.

0148-0227/08/2008JD009791$09.00

small bias between observations and model results [*O'Hirok and Gautier*, 2003].

[4] *Ramaswamy and Freidenreich* [1998, hereafter RF98] performed a detailed, high-spectral resolution study of near-infrared (NIR) solar flux absorption in cloudy atmospheres. Using idealized clouds they examined the effect of numerous factors, including vertical location, cloud thickness, solar zenith angle, and optical depth, on spectral atmospheric and surface fluxes. They found that the amount of NIR flux absorbed in the atmosphere depended strongly on cloud vertical location, while surface fluxes depended primarily on total cloud optical depth. In addition, they showed that the column atmospheric absorption is strongly driven by the amount of water vapor path above cloud top so that low clouds have a larger atmospheric absorption for the same cloud optical depth than high clouds and that optically thick high clouds can either increase or decrease the column absorption relative to clear sky, depending on their particle size.

[5] In this study, we focus on examining changes in the SW absorption in the tropical atmosphere associated with the vertical structure and diurnal variability of observed clouds. We extend previous theoretical studies [*Stephens*, 1978; *Lubin et al.*, 1996; *Ramaswamy and Freidenreich*, 1998] by examining the effect of clouds on absorption over the entire solar spectrum and by using high spatial and temporal resolution vertical profiles of cloud properties obtained from cloud radar observations at the Atmospheric Radiation Measurement (ARM) Tropical Western Pacific (TWP) sites on the islands of Manus, Papua New Guinea (2.06°S, 147.42°E), and Nauru (0.52°S, 166.92°E). We examine the column SW absorption and the vertical profiles of SW absorption calculated for observed clouds, including the contributions of observed cloud frequency, optical depth, vertical location, cloud overlap, and diurnal cycle. In our study, calculations of shortwave absorption at the ARM TWP sites indicate that, on average, the observed clouds increase the total column absorption by only a few W m^{-2} although they significantly change the distribution of absorption vertically in the column.

[6] We begin with a short description of the data and the radiative transfer model used in the study. This is followed by analysis of an idealized sensitivity test which illustrates some of the key radiative processes that govern the vertical distribution of shortwave absorption. Analysis of a case study and statistics from several months of observations illustrates how these processes are exhibited in observed clouds.

2. Data and Radiative Transfer Calculations

[7] Measurement capability at the ARM TWP sites includes twice-daily radiosonde launches, surface meteorology instrumentation, microwave radiometers that provide measurements of column integrated water vapor and liquid, and active remote sensing instruments (millimeter wavelength cloud radar, micropulse lidar, and ceilometers) that provide vertical distributions of hydrometeors [*Mather et al.*, 1998]. These measurements can be used to derive vertical profiles of atmospheric state (temperature, water vapor) and cloud properties (particle size, mass content), as described by *Mather et al.* [2007]. We examine several months of observations from Manus (February to July 2000) and Nauru (March to December 1999). Vertical profiles of temperature and water vapor are derived by combining radiosonde measurements with higher temporal resolution measurements of surface air temperature and total precipitable water vapor (PWV) from a microwave radiometer. Vertical profiles of cloud location, liquid/ice water content, and effective radius are retrieved from the 35 GHz cloud radar at 10-second temporal and 45-meter vertical resolution. Cloud phase (water, ice, or mixed) is determined from the temperature profile, with supercooled water allowed to exist down to −16°. For mixed phase clouds, the fraction of reflectivity associated with the ice and water components of the cloud is determined based on a linear function of temperature. Further details of the retrieved cloud properties are given by *Mather et al.* [2007].

[8] Radiative transfer calculations are performed on the retrieved cloud and atmospheric state profiles using the independent column approximation (ICA) in which each profile is treated as an independent column and there is no horizontal photon transport between columns. To reduce the time required for radiative transfer calculations without introducing artifacts caused by averaging the cloud properties, we sample the cloud property profiles every 5 minutes. Vertical profiles of broadband SW fluxes from 0.2 to 4.0 μm are calculated using a delta-four-stream correlated *k*-distribution radiative transfer model with 6 SW bands [*Fu and Liou*, 1992] with updated gaseous absorption coefficients based on the HITRAN 2000 database [*Rothman et al.*, 2003].

[9] Aerosols can affect the vertical distribution of SW absorption directly, through absorption of SW radiation by the particles themselves, or indirectly, through scattering of SW radiation that is then absorbed by water vapor or clouds in the atmosphere. In the current calculations, aerosols are neglected due to the low aerosol optical depths expected at the ARM TWP sites and the lack of information on the vertical distribution of aerosol. During 1999–2000 at Nauru, the average aerosol optical depth was 0.07 [*McFarlane and Evans*, 2004b] and large Angstrom coefficients indicate that coarse particles (likely nonabsorbing sea salt aerosol) dominate the aerosol properties at Nauru [*Smirnov et al.*, 2002]. At Manus, the aerosol optical depth and aerosol properties are more varied as Manus can be influenced by biomass burning aerosol transported from southeast Asia. However, the largest influence of biomass burning aerosol at Manus occurs during August–October [*Vogelmann*, 2002] while the current study examines data from February to July.

[10] Three sets of radiative transfer calculations are performed for each profile. The first set uses the retrieved cloud and atmospheric state profiles (CLD); the second set uses the same atmospheric state profiles but with no clouds (CLR); the third set uses the same cloud and atmospheric state profiles but removes absorption by hydrometeors within the cloud by setting the single scattering albedo to 1.0 at all wavelengths (NOCLDABS). Examining differences between the CLD and NOCLDABS cases allows us to separate the effect of the absorption by cloud particles from the effect of the cloud reflectivity on the gaseous absorption in the column.

[11] For nonprecipitating clouds, uncertainties in the retrieved ice water contents and ice particle sizes are

estimated to be a factor of 2, while uncertainties in retrieved liquid water properties are on the order of 10% [*Mather et al.*, 2007]. In the current study, precipitating clouds (which constitute 13% of the profiles at Manus and 3% at Nauru) are also included in the analysis. Precipitation below cloud base is neglected in the radiative transfer calculations by removing any radar reflectivity observed below the lidar-derived cloud base. For the precipitating clouds, the retrieved liquid water content and particle size are more uncertain as the retrieval techniques assume nonprecipitating clouds. In particular, cloud particle size is likely overestimated since the radar will be more sensitive to large drizzle or precipitation than to cloud particles. Liquid water content may also be overestimated since the microwave radiometer data cannot be used as a constraint if there is standing water on the radome.

[12] In previous work [*Mather et al.*, 2007] we calculated broadband fluxes using the same data set and methodology described above and compared the calculated fluxes to observed surface fluxes for clear-sky and nonprecipitating clouds to examine the accuracy of the radiative transfer model and the retrieved cloud properties. Differences between observed and calculated downwelling SW surface fluxes were less than 5% for all hemispherically clear sky cases, providing confidence in the radiative transfer model and atmospheric state inputs. Cloudy-sky comparisons showed greater scatter, and a bias toward underestimate of surface flux in the calculations, but the mean flux difference was around 5% of the observed surface flux at both sites, again indicating reasonable conference in the radiative transfer model and retrieved cloud properties. The larger differences for the cloudy sky cases are due to the lack of three-dimensional effects in the model, the uncertainty in the retrieved cloud properties, and the fact that cloud occurrence and microphysical properties were determined from vertically pointing instruments while SW fluxes are observed by instruments that have a hemispheric field of view (diffuse and total flux) or follow the sun (direct flux). Comparisons to observed SW TOA albedo from geostationary satellites were considerably worse than the surface flux comparisons, with little correlation between calculated and measured albedo. These differences are due primarily to the neglect of three-dimensional radiative effects and the spatial/temporal mismatch between the radar-derived cloud properties and the satellite fluxes.

3. Results

3.1. Sensitivity Analysis

[13] To illustrate the differing effects of low and high-level clouds on SW column absorption, we perform a simple sensitivity analysis. A detailed sensitivity analysis of near-IR absorption using a high-spectral resolution model and idealized clouds can be found in RF98. The results of the current sensitivity study, which uses a correlated *k*-distribution radiative transfer are consistent with the results presented in RF98 and are presented here for context in the discussion of the calculations using observed cloud structure and to extend the analysis to the full solar spectrum (0.2–4.0 μm). The current sensitivity analysis also illustrates the magnitude of errors in the absorption calculations associated with uncertainty in the retrieved cloud properties. We perform theoretical calculations using the average thermodynamic (temperature, pressure, water vapor) profile over the study period from the Manus site (column PWV = 5.4 cm), solar geometry of 21 March 2000, and homogeneous clouds with specified particle size, water path and cloud top height. Liquid clouds are assumed to have physical thickness of 500 m and ice clouds to have physical thickness of 3 km, which represent typical statistics observed at Nauru [*McFarlane and Evans*, 2004a]. In RF98, all modeled clouds were assumed to have liquid droplets; here high clouds are composed of ice particles, with optical properties specified by *Fu* [1996]. Additionally, the RF98 results were presented for instantaneous fluxes, while we primarily examine the diurnally averaged fluxes in our sensitivity study. Radiative transfer calculations are performed every 15 minutes, and the resulting fluxes are averaged over a 24-hour period.

[14] To determine the maximum effect on the daily-averaged column absorption, clouds are assumed to have 100% cloud cover. The SW absorption in the column is defined as the net (downwelling minus upwelling) SW flux calculated at the top of the atmosphere (TOA) minus the net flux calculated at the surface, assuming a surface albedo of 0.06. Column absorptance is defined as the column absorption divided by the incoming solar radiation at TOA. Clouds can affect SW column absorption in 3 ways:

[15] (1) Cloud particles absorb SW radiation, with the amount of absorption depending strongly on particle composition (liquid or ice) and particle size, and weakly on particle temperature.

[16] (2) Multiple scattering within a cloud increases the effective water vapor path length (and therefore the water vapor absorption) within the cloud.

[17] (3) SW radiation reflected from the top of a cloud can increase (decrease) the effective water vapor absorption path length if cloud top is lower (higher) than the majority of the column water vapor.

[18] The first two effects increase the amount of SW radiation absorbed in the column relative to the amount observed in a corresponding clear-sky column, while the third effect can increase or decrease the magnitude of SW column absorption relative to clear-sky, depending on the height of the cloud and the details of the water vapor profile. All of these effects change the vertical distribution of SW absorption in the atmosphere relative to clear sky. The second effect is smaller in magnitude than the other effects, and although it is included in the model calculations, it will not be examined in detail.

[19] The sensitivity calculations (Figure 1a) show that the enhanced SW column absorption relative to the clear sky due to tropical low-level (cloud top at 1.5 km) liquid clouds increases rapidly with liquid water path (LWP) for small values of LWP depth before it asymptotes to a nearly constant value at LWP > 250 g m^{-2}. For LWP > 100 g m^{-2}, the absorption by the cloud particles dominates the column absorption; for clouds with smaller optical depths, the increased water vapor absorption due to the reflected SW plays a larger role. The absorption of SW radiation by liquid droplets is dependent on particle size; larger droplets absorb more radiation than smaller droplets. For clouds with LWP > 100 g m^{-2}, where the absorption by cloud particles dominates the increase in water vapor absorption due to

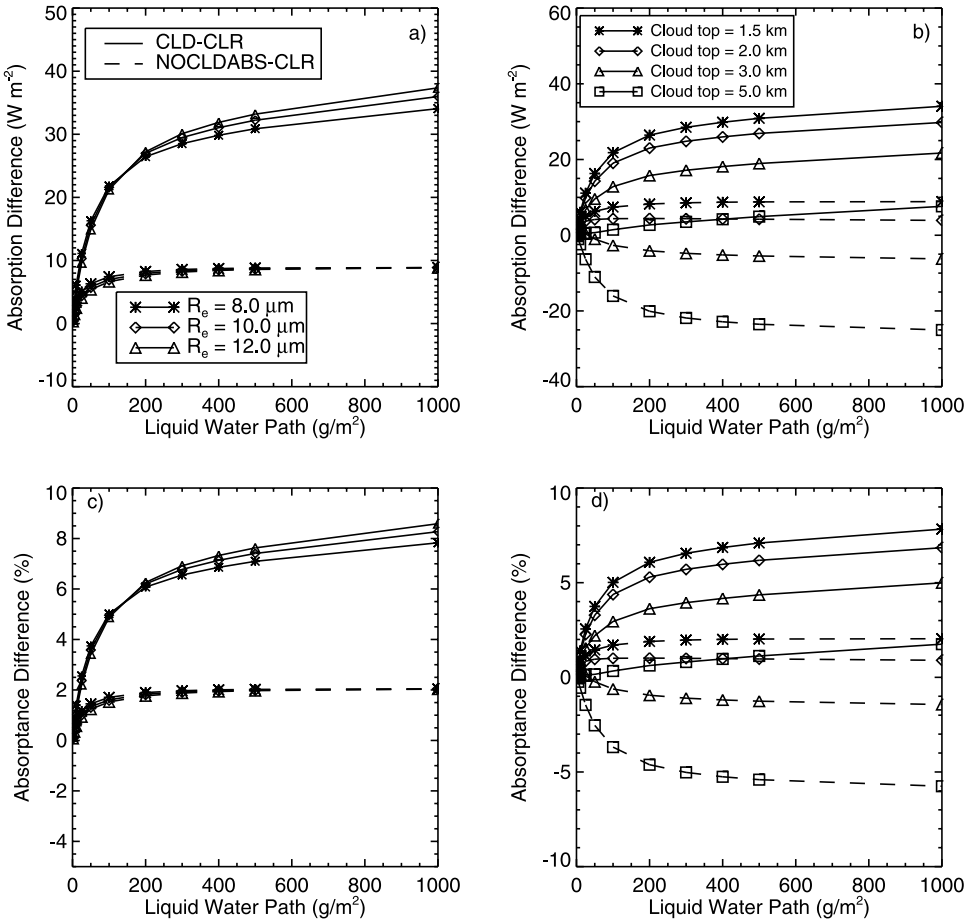

Figure 1. Diurnally averaged calculated CLD-CLR (solid line) and NOCLDABS-CLR (dashed line) column SW absorption (top) or absorptance (bottom) for homogeneous liquid water clouds with 100% cloud cover as a function of liquid water path and (a, c) effective radius or (b, d) cloud top height. Diurnally averaged clear-sky absorption for the given atmospheric conditions is 97.7 W m^{-2}.

reflection from cloud top, the clouds with 12 μm particles absorb approximately 10% more radiation relative to clear sky than the clouds with 8 μm particles. For clouds with lower LWP values, the increased reflectivity of the smaller particles leads to larger water vapor absorption which compensates for the reduced in-cloud particle absorption.

[20] The SW column absorption shows a strong dependence on cloud top height for these low-level clouds (Figure 1b). For liquid clouds with tops at 1.5 km, most of the column water vapor (WV) is above the cloud, therefore the reflection of SW radiation from cloud top increases the effective WV absorption path and increases the total column absorption. As the cloud top height increases, the percentage of the total column WV above the cloud decreases. The height at which the absorption of SW radiation by the cloud particles is offset by decreased water vapor absorption below the cloud due to the reflection of SW radiation from cloud top (here at 5 km) depends on the total amount of WV in the column and the structure of the WV profile, as well as details of the cloud microphysics.

[21] The sensitivity studies indicate that low tropical clouds increase column SW absorption relative to clear sky. The maximum calculated daily-averaged absorptance was 31% of the incoming radiation (for optically thick cloud with cloud top at 1.5 km and 12 μm droplets), compared to 23% of the incoming radiation absorbed in the corresponding clear-sky calculation. As cloud top height increases, the column absorption decreases, and midlevel liquid clouds may have slightly reduced column absorption relative to clear sky.

[22] For high-level ice clouds (cloud top >8 km), there is little dependence of column SW absorption on cloud vertical location (not shown) because of the small amounts of WV above cloud at these altitudes, but there is a strong dependence on ice water path (IWP) and particle size (Figure 2a). If there were no absorption of SW radiation by ice cloud particles (NOCLDABS calculation; dashed line), high-level ice clouds would always reduce the column absorption relative to clear-sky due to reflection of SW radiation. This reduction in column absorption increases with increasing IWP due to increased cloud reflectivity. However, the absorption of SW radiation by ice particles within the cloud offsets the reduction of water vapor absorption caused by cloud reflectivity. The magnitude of the offsetting absorption within the cloud depends on the ice water path of the cloud and the size of the ice crystals, since larger particles absorb more SW radiation.

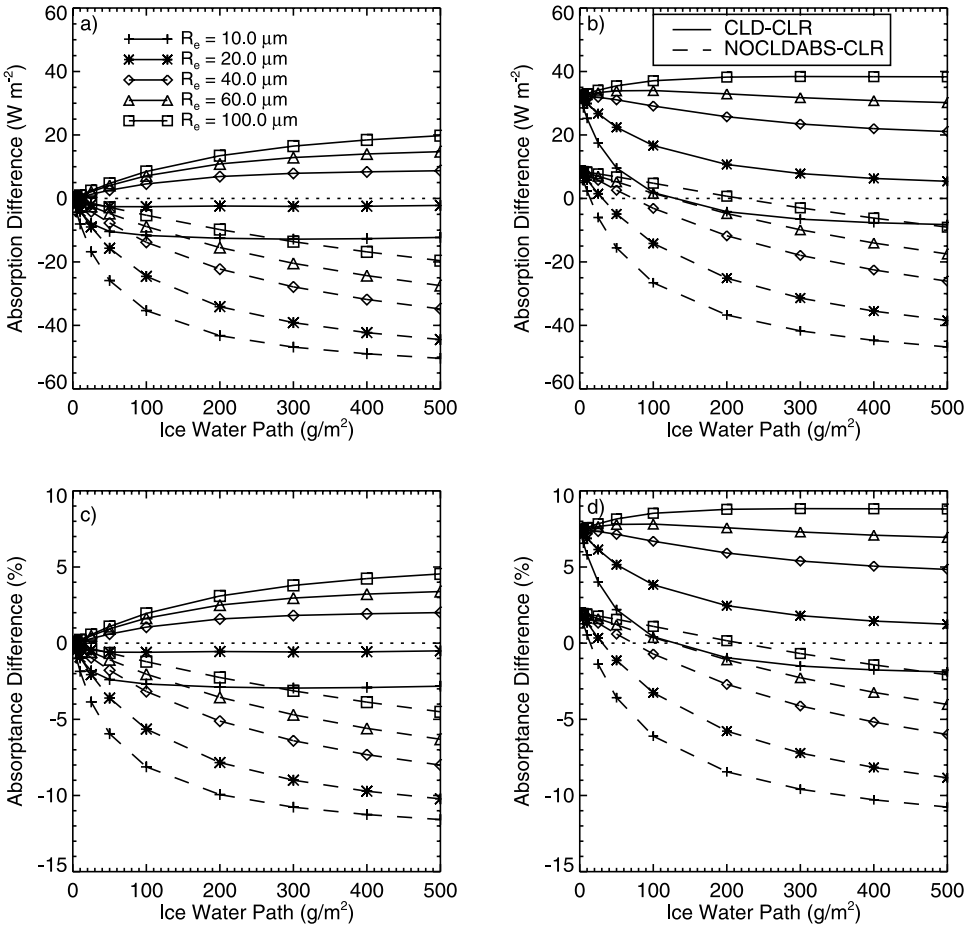

Figure 2. Diurnally averaged calculated CLD-CLR (solid line) and NOCLDABS-CLR (dashed line) column SW absorption (top) or absorptance (bottom) for (a, c) homogeneous ice water clouds with 100% cloud cover as a function of ice water path and effective radius and (b, d) multilayer clouds consisting of a high ice cloud with 100% cloud cover and varying effective radius and optical depth over an optically thick liquid water cloud with 100% cloud cover and fixed particle radius (8 μm), liquid water path (1000 g m^{-2}), and cloud top height (1.5 km). Diurnally averaged clear-sky absorption for the given atmospheric conditions is 97.7 W m^{-2}.

[23] In the Fu-Liou radiative transfer model, ice optical properties are parameterized assuming hexagonal crystals [*Fu*, 1996]. Details of the sensitivity tests vary when calculations are performed using optical properties of other crystal shapes (not shown), but the main conclusions are the same. For ice clouds with smaller particles (in this case, hexagonal crystals having effective radius less than approximately 40 μm) ice clouds reduce the column absorption relative to clear sky for all IWP values, reaching their maximum effect near IWP of 100 g m^{-2}. For ice clouds with larger particles the absorption in the ice cloud layer offsets the reduced water vapor absorption, leading to a net increase in column absorption for ice clouds with IWP > 10 g m^{-2}. For multilayer cloud scenes consisting of a high ice cloud over an optically thick low-level liquid cloud (Figure 2b), the effect on the column SW absorption again depends on the particle size and IWP of the ice cloud. Ice clouds with smaller particles partially reduce the increased column absorption due to the lower cloud, while ice clouds with larger particles have little impact on the total column absorption due to the compensating effects of particle absorption and reduced water vapor absorption.

[24] These sensitivity calculations impose a limit on the imaximum possible SW column absorption from the independent column approximation perspective (three-dimensional effects are discussed in section 4.2). For overhead sun, the maximum absorptance for an optically thick low-level cloud in the tropics is approximately 32% of the incoming solar radiation (Figure 3), compared to 23% for clear sky (an instantaneous difference of 156 W m^{-2} for the solar geometry used here). Clear sky absorptance increases with increasing solar zenith angle (SZA) for SZA > 20°, while liquid cloud column absorptance does not increase until SZA > 60°. The column absorptance difference (as well as total column absorption) is a maximum for overhead sun, and will be less for a diurnal average. Optically thick ice clouds with large particles have a maximum absorptance of 29% for overhead sun, but decrease to less than clear sky absorptance for SZA > 60° due to increased cloud reflectance. Ice clouds consisting of

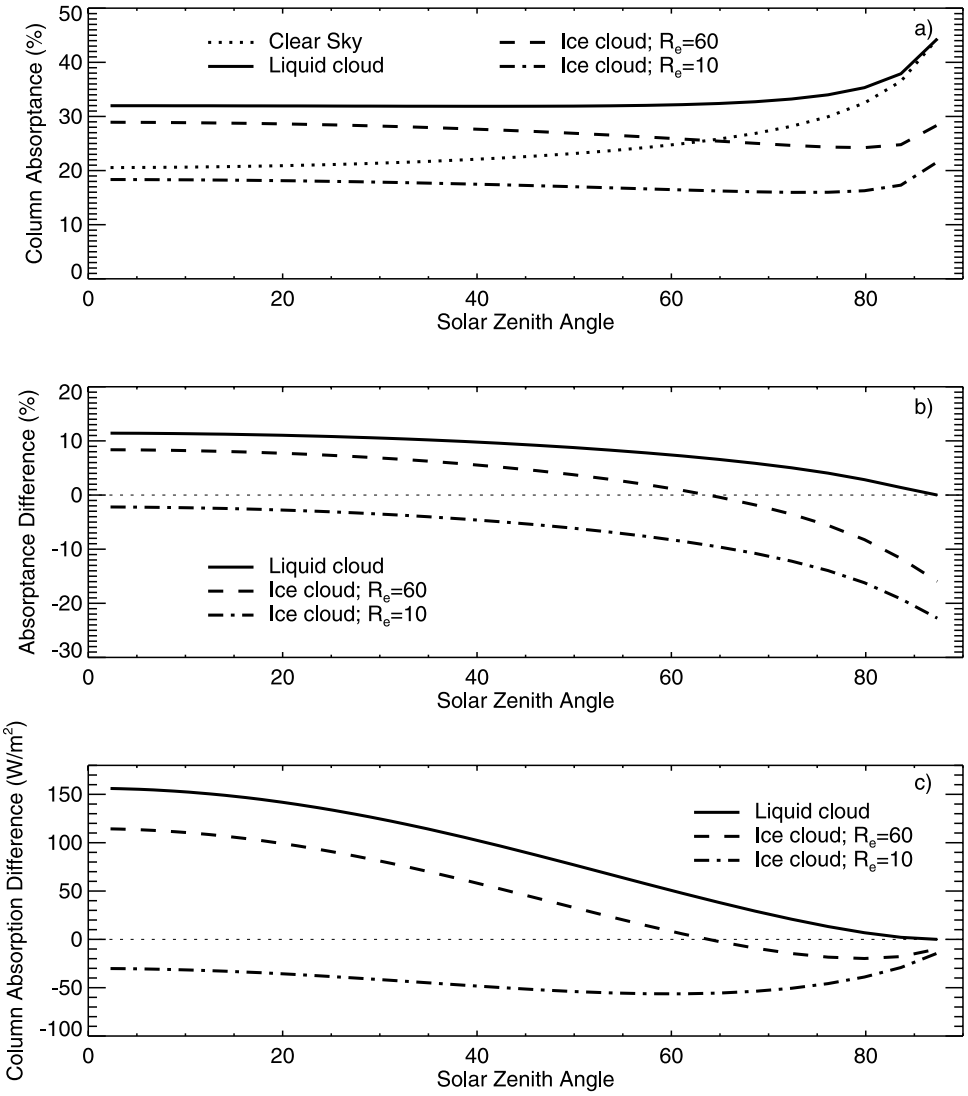

Figure 3. Maximum calculated (a) column absorptance, (b) column absorptance difference relative to clear sky, and (c) column absorption difference relative to clear sky as a function of solar zenith angle for idealized overcast clouds in the tropics using the independent column approximation.

small crystals have absorptance less than clear sky values for all solar zenith angles.

3.2. Case Study

[25] The sensitivity analysis examined the effect of idealized liquid and ice clouds on the total column SW absorption and illustrated that low-level clouds increase SW column absorption relative to clear sky, while high-level clouds tend to reduce column absorption except for ice clouds with large particles. The magnitude of the cloud effect on the column absorption depends on the optical depth, vertical structure, and frequency of occurrence of clouds. To illustrate the effects of observed clouds on the total column absorption and on the vertical distribution of absorption, we examine the results from a typical day with both high and low cloud (March 1, 2000) at the Manus site (Figure 4).

[26] The radar reflectivity image (Figure 4a) indicates a cirrus layer from 11 to 15 km and a layer of broken cumulus near 1 km. The cirrus layer has a radar cloud frequency of occurrence of 97% over the course of the day with a maximum optical depth of 7.0 and an average optical depth of 0.8, while the cumulus has cloud frequency of 26%, maximum optical depth of 31.0 and average optical depth of 5.7. Large differences in the SW column absorption between the CLD and CLR calculations are seen primarily during periods of low clouds (Figure 4b). Comparison with the NOCLDABS calculation (dotted line, Figure 4b) shows the enhanced water vapor absorption accounts for a significant fraction of the increased absorption during low cloud conditions. From approximately 1100 local standard time (LST) to 1330 LST there is little change in SW column absorption although there is persistent cirrus during this period; the reduction in water vapor absorption due to reflection from cloud top is offset by the absorption by the particles in the ice cloud. The NOCLDABS calculation for this time period indicates the large decrease in column absorption that would occur if there were no absorption by the cloud particles. During local morning (before 0900 LST) and evening (after 1600 LST) there is a decrease

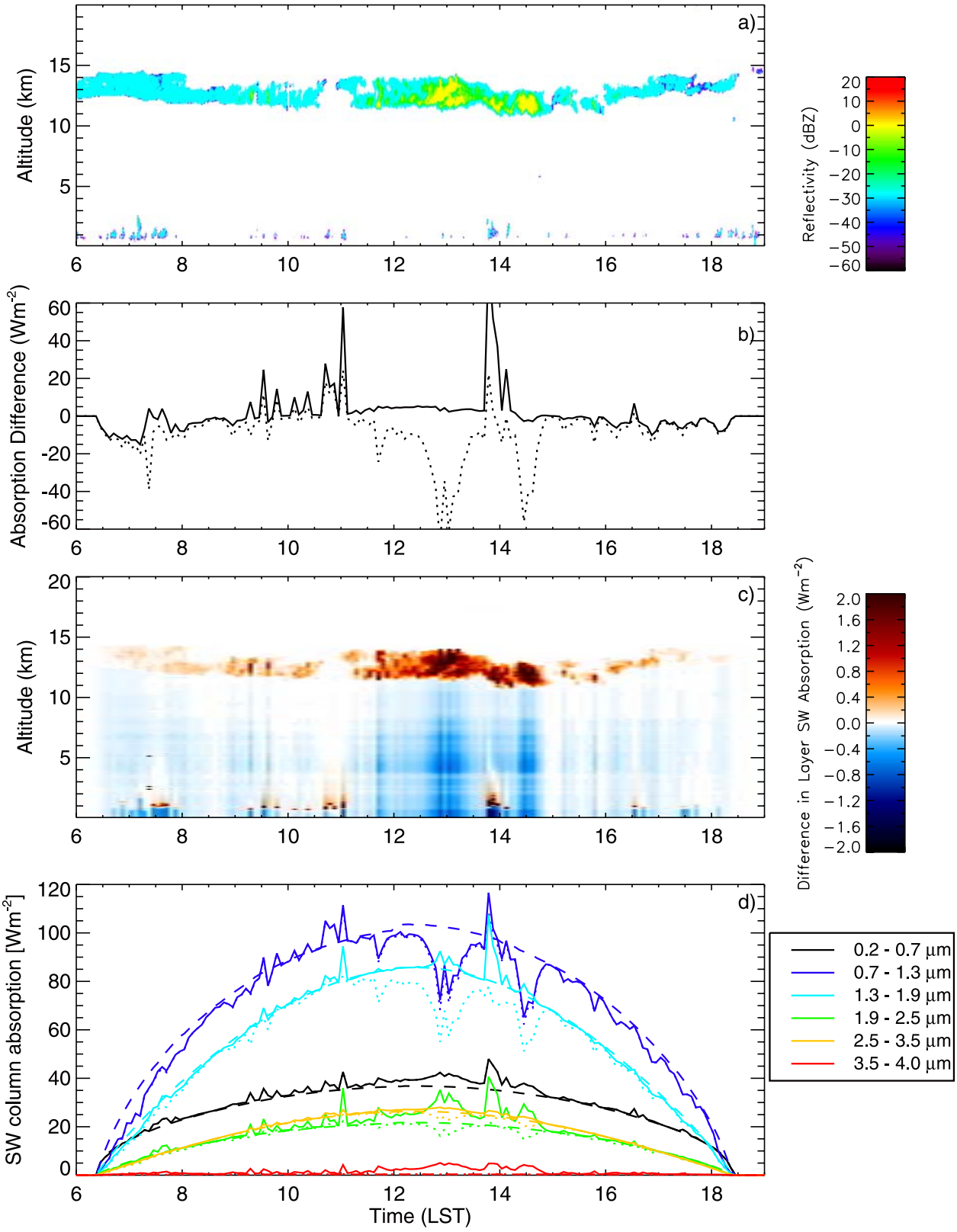

Figure 4. Case study from 1 March 2000 at Manus. Panels show (a) radar reflectivity, (b) difference in total column SW absorption for CLD-CLR (solid line) and NOCLDABS-CLR (dotted line), (c) difference in SW absorption in each 45-m layer (CLD-CLR calculation), and (d) amount of each spectral band absorbed in the column for CLD (solid line), CLR (dashed line), and NOCLDABS (dotted line) calculations.

Table 1. Details of the SW Bands and Optical Property Parameterizations in the Fu-Liou Correlated *k*-distribution Model

Wavelength, μm	Solar Constant, W m^{-2}	SSA water r_e = 10 μm	SSA ice r_e = 20 μm	SSA ice r_e = 60 μm
0.2–0.7	630.4	1.0000	1.0000	1.0000
0.7–1.3	487.1	0.9998	0.9993	0.9980
1.3–1.9	153.7	0.9886	0.9614	0.9037
1.9–2.5	51.1	0.9528	0.9294	0.8442
2.5–3.5	28.4	0.6426	0.6806	0.6349
3.5–4.0	5.5	0.8979	0.6908	0.5912

in total column SW absorption relative to clear sky, even during some periods when low cloud exists (near 0800 LST), due to the increase of cloud reflectivity at high solar zenith angles.

[27] Examination of the vertically resolved changes in SW absorption between the CLD and CLR calculations (Figure 4c) shows the absorption of SW radiation by cloud particles. Changes in absorption in the regions between the cloud layers are also evident. These changes are due to the reflection of SW radiation by the upper (lower) cloud and the resulting decrease (increase) in the amount of water vapor absorption in the column. Comparison of the radar reflectivity (Figure 4a) and the absorption difference (Figure 4c) clearly shows increased absorption (relative to clear-sky) in the lower troposphere above the low-level clouds and strong reductions in absorption below thick cirrus layers.

[28] The column absorption in each SW band for the given cloud scene is shown in Figure 4d for the CLD, CLR, and NOCLDABS calculations. Details of the spectral bands used in the radiative transfer calculations, including amount of incoming solar flux and typical values of single scattering albedo for ice and liquid particles in each band are given in Table 1. As seen in previous studies which used high resolution spectral models [*Lubin et al.*, 1996, RF98], there are large differences in the sensitivity of each band to the cloud properties.

[29] The shorter wavelength bands (0.2–0.7 μm and 0.7–1.3 μm) have the most incoming solar flux (82% of the TOA total downward solar irradiance), but little absorption by cloud particles (note high SSA in Table 1). Most of the change in column absorption due to cloud cover in these two bands is associated with changes in gas absorption due to reflection from clouds, as evidenced by the overlap of the CLD and NOCLDABS lines for these wavelengths. Most of the absorption in the 0.2–0.7 μm band is due to stratospheric ozone, so there is an increase in absorption for all cloud conditions. Most of the absorption in the 0.7–1.3 μm band is due to water vapor, so the sign of the absorption change depends on the cloud location. For the low cloud periods near midday, there is an increase in absorption. For high cloud periods, there is a decrease in absorption in this band.

[30] The bands exhibiting the highest sensitivity to cloud particle absorption are the 1.3–1.9 μm, 1.9–2.5 μm and 3.5–4 μm bands. The first two of these bands exhibit a significant amount of gaseous absorption (50–60% of incoming SW at TOA is absorbed in the clear sky column) while the 3.5–4 μm band is in an atmospheric window so there is little gaseous absorption. There is relatively little energy in these bands with 11.3%, 3.8%, and 0.4% respectively of the TOA total downward solar irradiance. The 2.5–3.5 μm band is almost completely saturated by gaseous absorption (>90% of incoming SW at TOA is absorbed in the clear sky column) so has little sensitivity to cloud change. The fact that the greatest sensitivity of column absorption due to cloud particles corresponds to regions of the solar spectrum containing a small portion of the total solar energy significantly limits the possible impact of clouds on the total column solar absorption.

3.3. Average Absorption at Manus and Nauru

[31] We now examine the statistics of the column integrated and vertical distribution of SW absorption at Manus (February to July 2000) and Nauru (March to December 1999). Due to the difficulty of operating active remote sensors in the tropical environment, there are frequent periods of missing cloud data, for which fluxes cannot be calculated. Daily (24 hours) averages are calculated only if at least 95% of the daytime cloud data exists (92 days at Manus and 252 days at Nauru). The daily-averaged SW column absorption values for CLR and CLD calculations at Nauru and Manus are shown in Figure 5a with the mean and range given in Table 2. As shown in previous studies [*Stephens*, 1978; *Stephens and Tsay*, 1990], clouds produce

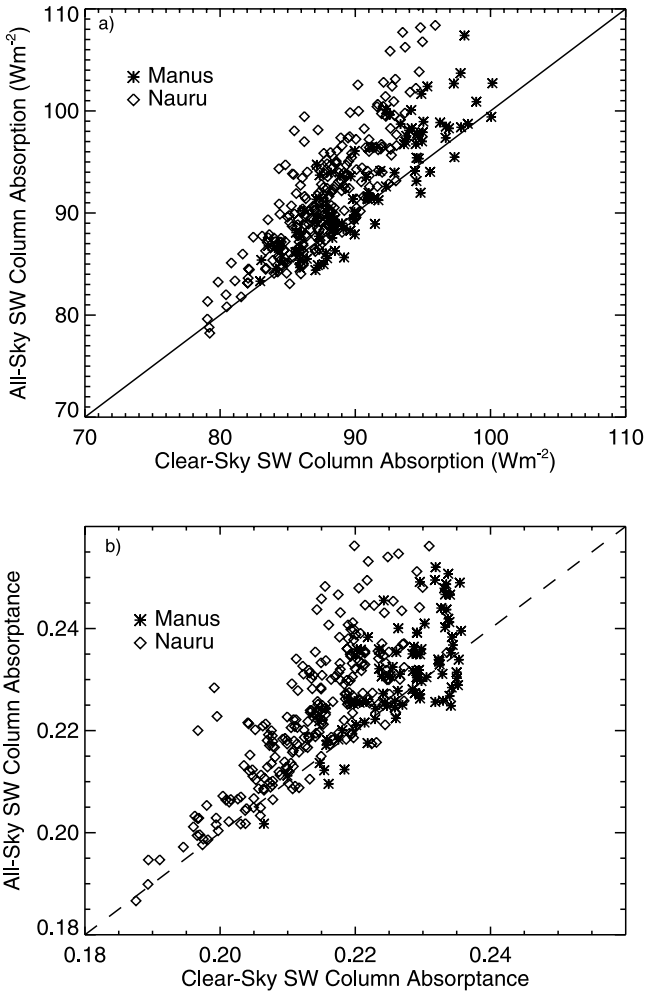

Figure 5. Daily-averaged SW (a) column absorption and (b) column absorptance for CLD and CLR calculations at Manus (stars) and Nauru (diamonds) for all days with at least 95% observed cloud data.

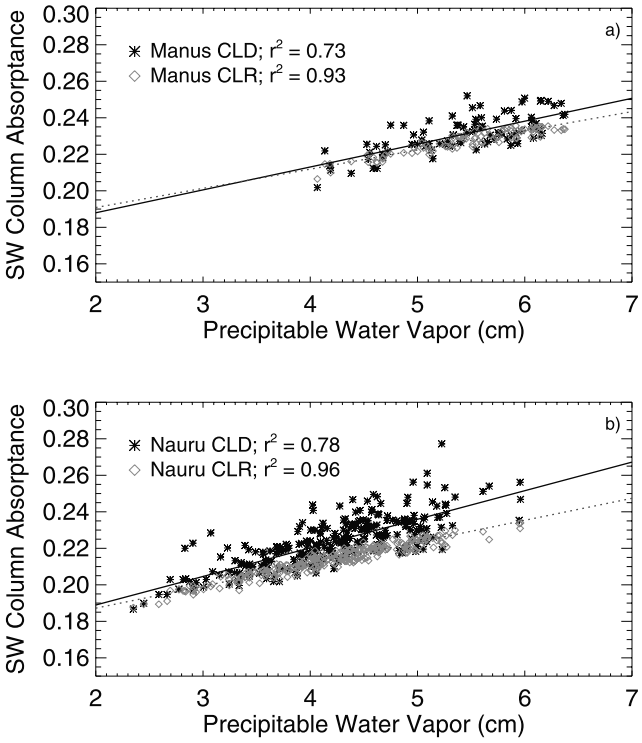

Figure 6. Calculated daily average SW column absorptance as a function of PWV for each day with at least 95% observed cloud data at (a) Manus and (b) Nauru. Solid and dotted lines are linear fits to the CLD and CLR data, respectively.

little change in the mean column-integrated atmospheric absorption. The average difference between the calculated CLD and CLR SW column absorption is only 1.6 W m^{-2} at Manus (2% of average clear-sky value) and 4.0 W m^{-2} at Nauru (5% of average clear-sky value). The range in the clear-sky column absorption is due primarily to seasonal variability in the total downwelling flux at TOA as well as variability in the total precipitable water vapor (PWV) column amount. By examining SW absorptance (Figure 5b), rather than absorption, the effect of the variability in incoming SW at TOA with time of year is removed. The SW calculated clear-sky column absorptance is strongly controlled by the total amount of PWV in the column (Figure 6a), and the column PWV also plays a large role in the variability of the calculated all-sky absorptance. The range in all-sky absorptance due to the range of observed PWV is larger than the range in all-sky absorptance due to differences in cloud amount and cloud properties for a given PWV value.

[32] The sensitivity tests illustrate that optically thick low clouds with 100% cloud cover can increase the daily-averaged column absorption by 30 W m^{-2} relative to clear sky or increase daily average absorptance by 9%. However, the average absorption differences calculated at the Nauru and Manus sites using the retrieved cloud vertical profiles are dramatically smaller (Table 1). Below we discuss several reasons for this result.

[33] At an instantaneous point in time, the observed clouds can significantly affect the column SW absorption as expected; the maximum instantaneous differences in CLD-CLR absorption calculations over the study period are 142.3 W m^{-2} at Manus and 164.8 W m^{-2} at Nauru. However, at the two TWP sites, the low cloud frequency is generally less than 50% (average daytime low cloud frequency from the radar observations is 39.3% at Manus and 42.8% at Nauru). Additionally, the low clouds observed at Manus and Nauru are not always optically thick, which will reduce their absorption; the average liquid water path of retrieved liquid clouds is 128.7 g m^{-2} at Manus and 39.8 g m^{-2} at Nauru. Based on these two factors alone, we would expect to observe significantly less than the maximum daily-averaged difference found in the sensitivity studies.

[34] Another factor in the small daily-averaged differences is the presence of ice clouds. The sites have similar frequency of liquid cloud but Manus has a larger frequency of high cloud (60.3%) than Nauru (23.0%) during the study period, which results in a higher frequency of multilayer cloud scenes. When cirrus cloud occurs above low cloud, the effect of the low cloud on the column absorption is reduced because the large reflectance of SW radiation at the top of the ice cloud results in less solar radiation reaching the lower cloud. Additionally, the diurnal signature in absorption is stronger when high cloud is present, because the reduction in WV absorption due to reflection from cloud top increases at higher SZA as cloud reflectivity and photon path length increase.

[35] The effect of ice clouds can be seen by examining the daily average absorption as a function of ice cloud

Table 2. Statistics of 24-hour Averaged SW CLD and CLR Column Absorption (Absorptance) Calculations at Manus and Nauru for Days With at Least 95% of the Daytime Cloud Observations Existing[a]

	Manus		Nauru	
	CLR	CLD	CLR	CLD
Mean SW absorption (absorptance)	91.5 W m^{-2} (22.7)	93.3 W m^{-2} (23.1)	87.2 W m^{-2} (21.4)	91.3 W m^{-2} (22.4)
Min SW absorption (absorptance)	83.3 W m^{-2} (20.6)	84.3 W m^{-2} (20.2)	74.6 W m^{-2} (18.8)	78.0 W m^{-2} (18.7)
Max SW absorption (absorptance)	99.9 W m^{-2} (23.6)	107.0 W m^{-2} (25.2)	95.7 W m^{-2} (23.4)	118.0 W m^{-2} (27.7)
Mean difference in absorption (absorptance)	1.6 W m^{-2} (0.4)		4.0 W m^{-2} (1.0)	
Min difference in absorption (absorptance)	−3.4 W m^{-2} (0.9)		−2.1 W m^{-2} (0.5)	
Max difference in absorption (absorptance)	9.3 W m^{-2} (2.1)		23.1 W m^{-2} (5.4)	

[a]Differences are given in terms of CLD-CLR.

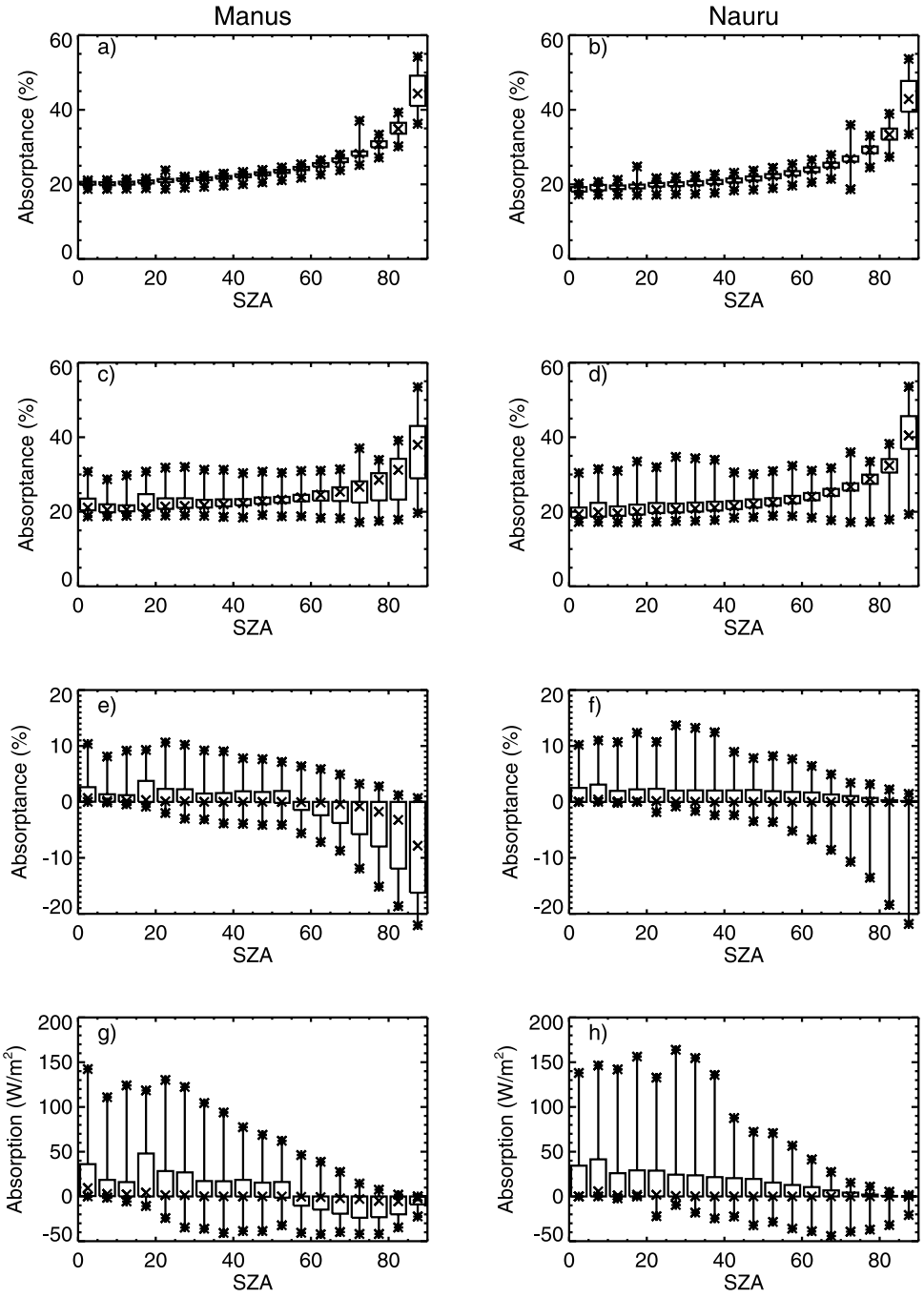

Figure 7. Calculated column absorptance or absorption as a function of solar zenith angle at Manus (left) and Nauru (right). (a and b) CLR column absorptance, (c and d) CLD column absorptance, (e and f) CLD-CLR column absorptance, (g and h) CLD-CLR column absorption. In each SZA bin, median values are shown by crosses; the boxes represent the 25% and 75% quartile values, and the lines and stars indicate the minimum and maximum values.

frequency. Nauru shows a strong positive correlation (0.83) between the daytime frequency of liquid cloud and the daily average difference between CLD and CLR absorption, while Manus has a much weaker correlation (0.40). At Nauru, during this period, 59% of the days have ice cloud frequency less than 20%, compared to only 20% of the days observed at Manus. If only these days are examined, the correlation between daytime liquid cloud frequency and column absorption difference increases at both Nauru (0.90) and Manus (0.60), illustrating how multilayer cloud affects the absorption differences. Both sites show weak negative correlation (−0.24 at Nauru; −0.08 at Manus) between daytime frequency of ice cloud and column absorption difference. If only the few days (8% at Nauru, 19% at Manus) with liquid cloud frequency <20% are examined, the negative correlations are much stronger (−0.58 at Nauru; −0.41 at Manus).

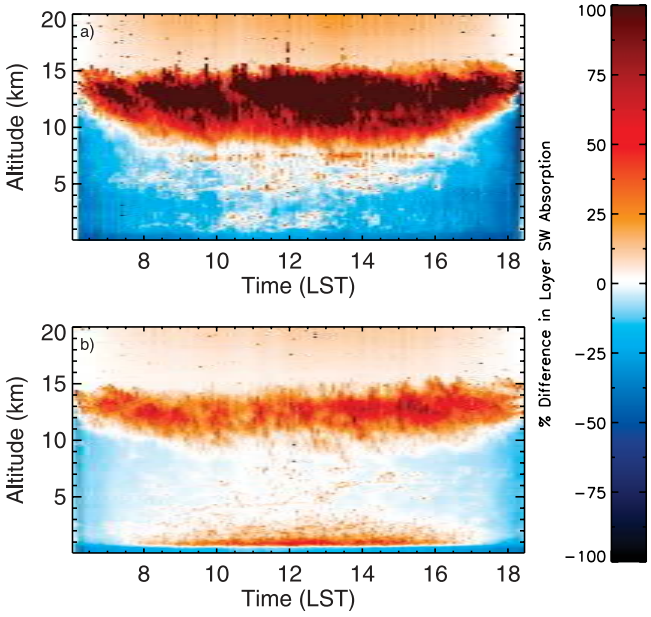

Figure 8. Average percentage change in (45-m thick) layer shortwave absorption due to clouds at (a) Manus and (b) Nauru. Difference in layer absorption is given as (CLD − CLR) / CLR.

[36] Examining only the daily-averaged difference masks the significant diurnal variability seen in the calculated column absorptance. Both the calculated all-sky and clear-sky column absorptance values show a strong diurnal signal, with median absorptance increasing with increasing solar zenith angle (Figure 7). For a given solar zenith angle, the all-sky calculations have significantly more variability than the clear-sky calculations. However, the central two quartiles (the boxes) are tightly grouped even for the CLD cases. At Manus, there is also a strong diurnal signal in the absorptance (and absorption) differences. For SZA < 60°, the median differences are small, but positive while for SZA > 60° the all-sky calculation tends to have smaller absorptance than the clear-sky column so the median differences are negative. Over the diurnal average, the reduced absorption relative to clear-sky at high SZA will offset some of the increased absorption at low SZA, reducing the daily average absorption difference. At Nauru, the minimum absorptance difference shows much less variability with SZA than Manus. Both sites show similar envelopes in the minimum/maximum absorptance with solar zenith angle, indicating that the main differences in the median absorptance are in the reduced frequency of high cloud at Nauru.

[37] The above analysis indicates that the small differences in calculated daily-averaged all-sky and clear-sky absorption at Manus and Nauru are due to less than 100% low cloud cover at both sites, low clouds that are not optically thick (primarily at Nauru), and the frequent presence of ice clouds (primarily at Manus). The larger difference between daily-averaged all-sky and clear-sky absorption at Nauru relative to Manus, and the lack of a strong signature in the median absorptance differences is due primarily to the much reduced frequency of high cloud at Nauru relative to Manus.

[38] Although the average effect of clouds at Nauru and Manus on the total column SW is small, they have a large impact on the average vertical distribution of SW absorption within the column (Figure 8). The impact of clouds on the vertical and diurnal distribution of SW absorption is very different at the two sites because of the significant differences in high cloud frequency at the two sites. At both sites, clouds strongly decrease the SW absorption in the lowest 1 km of the atmosphere and increase the absorption above 15 km. At Manus, clouds tend to strongly increase the SW absorption from 8–15 km and weakly increase the absorption between 5–8 km. Although Manus has more and optically thicker low clouds than Nauru (average low cloud liquid water path at Manus is 128.7 g m^{-2}, compared to 39.8 g m^{-2} at Nauru), the low clouds only weakly increase the absorption from 1–3 km during the middle of the day because of the frequent high cloud cover. At Nauru, clouds tend to strongly increase the SW absorption from 1–3 km and from 10–14 km throughout much of the day, and weakly increase the SW absorption from 3–10 km during the middle of the day.

[39] The daily composite of SW absorption due to clouds also illustrates the average effect of the diurnal cycle. During the early morning and late afternoon hours when solar zenith angles are lower, there is increased reflection from high clouds, and the SW absorption in the lower troposphere is decreased relative to clear sky at both sites. The diurnal effect is much stronger at Manus.

4. Discussion

4.1. Uncertainties in Calculated Absorption

[40] One of the primary sources of uncertainty in the calculated absorption profiles is in the retrieved profile of ice crystal size. If the particle size retrievals are biased low (high), the calculated ice cloud absorption could be underestimated (overestimated). The sensitivity tests performed in section 3 illustrate that there is approximately 10 W m^{-2} difference in the column absorption associated with a factor of two difference in ice crystal particle size for an optically thick ice cloud although this difference is smaller for optically thin clouds. The retrieval of ice crystal properties from remote sensing measurements is a subject of current research [e.g. *Comstock et al.*, 2007, and references therein]. In the current study, ice crystal size is based solely on temperature (particle size increases with increasing temperature) using a parameterization developed from in situ aircraft data taken in midlatitude clouds [*Ivanova et al.*, 2001]. A wide range of parameterizations of ice crystal effective radius as a function of temperature [*Ivanova et al.*, 2001; *Garrett et al.*, 2003] or temperature and ice water content [*McFarquhar*, 2001; *Sun and Rikus*, 1999] derived from in situ aircraft observations exist in the literature. Due to the uncertainties associated with in situ measurement of nonspherical ice crystals, including possible artifacts in size distribution measurements [*McFarquhar et al.*, 2007], it is unclear which is the most accurate. Based on the range of parameterization coefficients in the above studies, we estimate the uncertainty in the retrieved particle size to be approximately a factor of two.

[41] There is also uncertainty in the calculated column absorption due to the assumption of hexagonal ice crystals

in the calculations. In situ observations have shown that cold clouds often contain bullet rosettes or a mixture of particle shapes. There is little sensitivity of SW broadband ice crystal absorption to crystal shape [*Wyser*, 1999], however the asymmetry parameter does depend on crystal shape. The asymmetry parameter determines the amount of forward scattering and hence affects the reflectivity of the ice cloud and thus the total column absorption. *Wyser* [1999] found that the difference in net flux calculated using various crystal shapes compared to that calculated using ice spheres was generally less than 10%, except for aggregates which had flux differences of 15–20%.

[42] A further source of uncertainty is the use of the independent column approximation (ICA) to calculate the absorption profiles. Estimates of the magnitude of biases in absorption from using the ICA rather than full three-dimensional radiative transfer calculations differ depending on the horizontal domain, the assumptions made, and the cloud types and geometries studied [*Barker et al.*, 1998; *Fu et al.*, 2000; *DiGiuseppe and Tompkins*, 2003]. To address this issue, *DiGiuseppe and Tompkins* [2005] performed a systematic study of the three-dimensional effect in tropical convective regimes by using an idealized function to vary the anvil cloud fraction produced by a cloud resolving model without significantly altering the geometric structure or horizontal variability. They found that one-dimensional radiative transfer errors were a maximum at anvil cloud fractions of 30%, and were greatly reduced for larger cloud fractional cover. In all cases, one-dimensional theory underestimated the amount of absorption in the column relative to the three-dimensional calculations. The error in absorption was largest for overhead sun, with a maximum error of 30% for cloud fractions near 30%, and decreased with increasing solar angle to 20% at solar zenith angle (SZA) of 60 and 10% at SZA of 75.

[43] Analysis of Geostationary Meteorological Satellite (GMS) cloud retrievals [*Nordeen et al.*, 2001] at 0.3° resolution over a $5° \times 5°$ area around the Manus and Nauru sites indicates that the cloud fraction was 10–50% only 23% of the time at Manus from January–July 2000 and only 20% of the time at Nauru from June–December 1999. Therefore the errors in the ICA absorption calculations are most likely smaller than the maximum given in the *DiGiuseppe and Tompkins* [2005] study.

4.2. Vertical Distribution of Absorption

[44] The results presented in the preceding section indicate that clouds significantly alter the vertical distribution of SW absorption in the tropical atmosphere, even if they do not have a large impact on the average column absorption. Details of the vertical distribution of the SW absorption depend on the characteristics of the observed cloud and water vapor profiles. The radiative budget in climate models is usually evaluated by comparison to TOA and surface radiation measurements. Due to the offsetting impacts of low- and high-level clouds on the column absorption, atmospheric columns with very different cloud vertical structures may have similar column integrated absorption yet have different impacts on cloud-scale and large-scale dynamics.

[45] Modeling studies have indicated the importance of the diurnal cycle of absorbed shortwave radiation to the diurnal cycle of tropical oceanic convection and precipitation [*Xu and Randall*, 1995; *Kubota et al.*, 2004]. These analyses have primarily focused on the role of SW heating of anvil cloud layers, however *Kubota et al.* [2004] emphasize that the diurnal cycle of boundary layer cloud radiative heating is also important to the diurnal cycle of convection. This emphasizes the importance of understanding the vertical resolution at which cloud property and heating profiles need to be resolved to accurately predict the effects of radiative heating in clouds on the large scale dynamics. A study by *Wang and Rossow* [1998] also illustrated a significant impact on the Hadley circulation in the GCM when clouds with the same total optical depth and vertically integrated net radiation are split into two model layers rather than one model layer due to the impact of differential longwave heating/cooling at cloud base/top.

[46] Many GCMs do not have sufficient horizontal or vertical resolution to resolve shallow boundary layer cumulus or midlevel clouds and may neglect important details of vertical radiative and latent heating structures, which impact simulation of dynamical features such as the Madden-Julian Oscillation (MJO; [*Inness et al.*, 2001]). Comparisons of modeled cloud profiles with those observed from ground-based radars have identified differences in observed and modeled cloud vertical structure, due in part to the coarse vertical resolution in the models, that affect the model heating rate profiles [*McFarlane et al.*, 2007]. In particular, the peak in boundary layer cloud heating and cooling was broader and higher in the atmosphere in the average GCM profiles than in the observed profiles, which could affect boundary layer dynamics. Studies that systematically explore the effects of cloud vertical structure and vertical resolution on radiative and latent heating profiles, and the subsequent impact on dynamics, are needed to explore this issue. Although ground-based cloud radars exist at only a few sites around the world, the cloud profiling radar on the CloudSat satellite will provide global profiles of cloud properties and associated heating rate profiles for model evaluation.

4.3. Variability of SW Absorption

[47] As illustrated in the comparisons between the Manus and Nauru sites, the frequency of occurrence of various cloud types has a strong impact on the vertical distribution of SW absorption, as well as an impact on the total column absorption. Optically thick liquid clouds have the largest impact on the total column absorption. At the tropical sites studied, there was generally less than 50% low cloud cover and most low clouds had $\tau < 50$. The frequent cirrus cover at Manus reduced the impact of the low clouds on the column absorption while amplifying the diurnal cycle in SW absorption. Large differences were seen in the vertical distribution of SW absorption at the two sites due to the differing frequencies of high clouds, indicating that the absorption profiles will vary with intraseasonal, annual, and interannual cycles of convection in the tropics such as the Madden-Julian Oscillation, the migration of the intertropical convergence zone, and the El Nino–Southern Oscillation. Regions of the globe with more extensive and optically thick low cloud (such as subtropical stratocumulus regions) or less cirrus may show larger changes in column absorption relative to clear sky and larger impacts on the

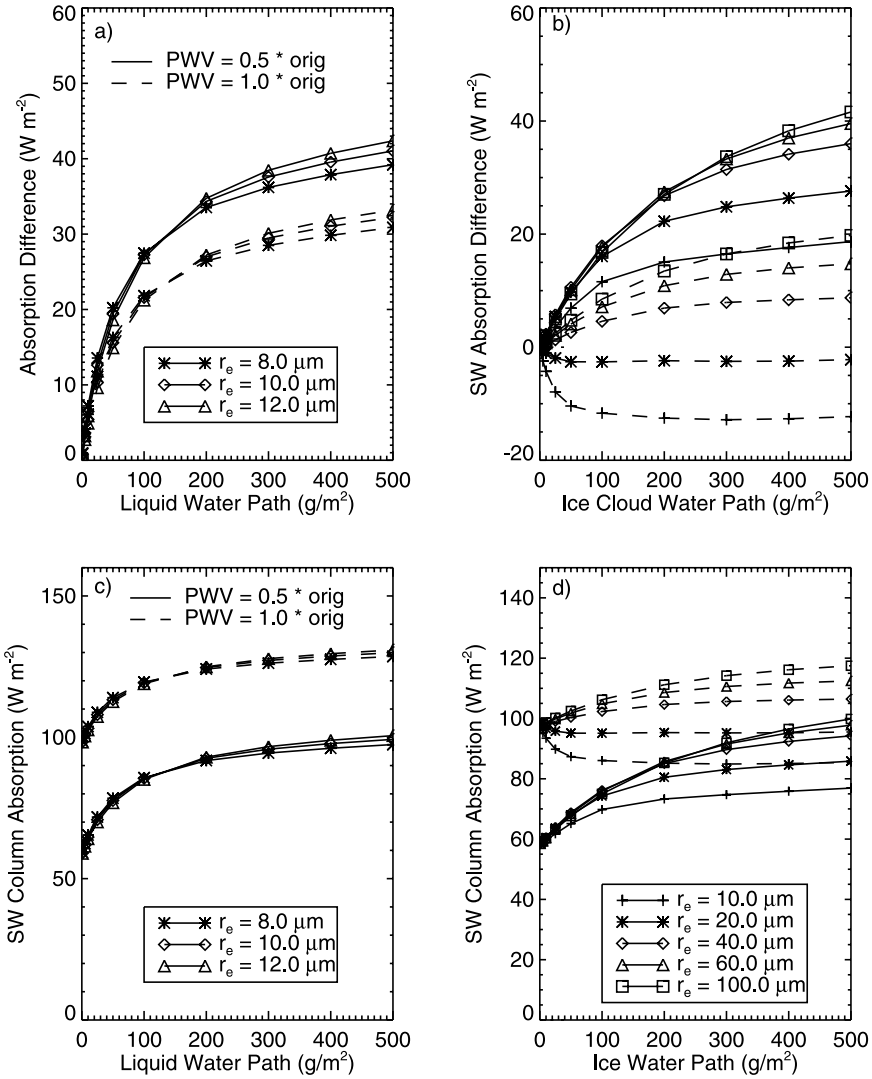

Figure 9. (top) Difference between daily-averaged CLD and CLR column absorption as a function of column precipitable water vapor and water path for idealized (a) liquid clouds and (b) ice clouds. (bottom) Daily-averaged SW column absorption for CLD calculations as a function of column precipitable water vapor and water path for idealized (c) liquid and (d) ice clouds. Liquid clouds have tops at 1.5 km and ice clouds have tops at 9 km.

vertical distribution of absorption in the boundary layer and lower troposphere than were seen at these tropical sites.

[48] Another feature of the tropical atmosphere that plays a large role in the effect of clouds on the SW absorption is the large column water vapor amount. For columns containing ice cloud, absorption by the cloud particles is often completely offset by the large decrease in water vapor absorption in the column due to reflection from cloud top. In regions with lower water vapor amounts, the absorption within the ice cloud might be significantly larger than the reduction in water vapor absorption in the column. To investigate the role that the large water vapor column in the tropics plays in the results presented here, we perform similar theoretical calculations to those presented in section 3.1, but reduce the column PWV to 2.5 cm, which is similar to column water vapor amounts seen in the midlatitudes. Observations of clouds at the ARM Southern Great Plains site in Oklahoma indicate that midlatitude ice clouds are often physically thick, with half of radar observed ice clouds having physical thickness >2 km [*Wang and Sassen*, 2002]. For a detailed examination of the differences between column absorption in tropical and midlatitude clouds, calculations using observed midlatitude water vapor and cloud profiles are needed. However, even this simple analysis illustrates the importance of the column water vapor amount on cloudy-sky column absorption.

[49] Comparisons between these sensitivity tests (Figure 9) illustrate that in an atmospheric column with reduced total WV, ice clouds are more likely to increase the total column absorption relative to clear sky. Liquid clouds in the lower WV environment also show a larger increase in column absorption relative to clear sky than in the original sensitivity tests. In the high WV environment, some of the water vapor absorption bands in the model are saturated and the absorption (relative to clear sky) is not as enhanced by the doubled water vapor path due to cloud top reflection as it is

in the lower WV atmosphere. The total column absorption in the tropical atmosphere is higher for all conditions than that in the reduced WV atmosphere (Figures 9c and 9d), although for optically thick ($\tau > 20$) ice clouds, the total column absorption is similar for the tropical and midlatitude WV amounts. Due to the high water vapor amounts in the tropical atmosphere, the effects of high ice clouds on the total column absorption may counteract that of low-level clouds, leading to little change in total column absorption relative to clear sky although the vertical distribution of SW absorption is affected. In regions with lower WV amounts, ice clouds are more likely to increase total column absorption relative to clear sky. The variability in SW absorption associated with differences in cloud vertical structure and variations in water vapor profiles indicate that changes in cloud properties are likely to lead to regionally dependent dynamical and hydrologic effects [e.g., *Wang and Rossow*, 1998; *Erlick et al.*, 2006].

4.4. Implications for Surface/Satellite Closure Studies

[50] The results in Figure 3 show that the theoretical maximum SW absorption enhancement due to clouds is about 30% (similar to the value seen in Figure 2b of RF98). Achieving this maximum requires optically thick low clouds with 100% cloud cover and no high clouds. Such cloud conditions rarely, if ever, occur in the tropical western Pacific. Figures 5 and 6 demonstrate that the average calculated SW absorption for actual all-sky conditions is only marginally greater than that for clear sky conditions. The mean daily-average absorption difference is only 1.6 W m^{-2} at Manus and 4.0 W m^2 at Nauru and the range in daily-average column absorption is 84.3 W m^{-2} to 118.0 W m^{-2}.

[51] These results are consistent with the majority of theoretical studies, which have shown no evidence for the large cloud absorption claimed by the *Cess et al.* [1995] study. Recent work by *Kim and Ramanathan* [2008], in which satellite-derived global cloud and aerosol properties were input into a one-dimensional radiative transfer model, found that annual global mean all-sky SW column absorption was 79 ± 5 W m^{-2}, compared to 72 ± 3 W m^{-2} for clear-sky. Given the stated uncertainties, the effect of clouds on column SW absorption is the same order of magnitude found in our study. The *Kim and Ramanathan* [2008] study finds good agreement between calculated all-sky fluxes and observed fluxes at the surface and TOA on monthly-mean timescales, indicating consistency between the input cloud properties, calculated absorption, and surface and satellite fluxes.

[52] Previous studies of surface fluxes derived from satellite measurements have indicated that most differences between point measurements at the surface and satellite area-mean retrievals are due to sampling errors; that satellite-derived and observed surface fluxes agree well on monthly mean timescales; and that agreement improves as more surface flux observations are included in the average [*Li et al.*, 1995, 2005]. These results indicate that the spatial mismatch between surface and satellite observations and three-dimensional effects such as horizontal transport of photons out of the observed column need to be carefully accounted for at shorter timescales. *Barker and Li* [1997] addressed the issue of using satellite/surface observations to estimate column absorption at 1-hourly timescales. Using three-dimensional radiative transfer modeling, they found that for nonuniform clouds, the effects of horizontal transport of radiation out of the column and poor sampling of transmittance at the surface created 'apparent' absorption when satellite and surface flux observations were combined. Similarly, *Fu et al.* [2000] compared atmospheric absorption in each column as calculated from three-dimensional Monte Carlo radiative transfer simulations to the column absorption calculated from the difference between the calculated net TOA and surface fluxes. Although the domain averaged absorption was the same in both methods, the ''apparent'' absorption calculated from the TOA and surface fluxes had significant error on a column-by-column basis, including large overestimates and underestimates.

[53] In a preliminary analysis, we calculated SW column absorption from daily-averaged satellite and surface observations over the Manus site (Figure 10). The TOA broadband fluxes over Manus were derived from the Geostationary Meteorological Satellite (GMS-5) at 0.3° resolution [*Nordeen et al.*, 2001]. The satellite retrievals provided shortwave TOA broadband clear-sky and all-sky albedo as hourly values. For consistency, TOA albedo was converted to SW upwelling flux using the same solar constant used in the radiative transfer model calculations, and net TOA flux was calculated as incoming flux at TOA minus upwelling flux at TOA. The hourly shortwave net fluxes were integrated from sunrise to sunset and averaged over 24 hours to give the daily-averaged net fluxes. Missing TOA shortwave fluxes were filled in with an average of nearby values at the same local time and days with more than 4 hours of missing data were removed from the analysis. Daily-averaged all-sky downwelling surface fluxes were calculated from 1-min pyranometer observations and clear-sky fluxes were estimated from the methodology of *Long and Ackerman* [2000]. Net surface flux was calculated by assuming a constant surface albedo of 0.06. Then column absorption was defined as the difference between the TOA net flux and the surface net flux.

[54] On average over the study period, the all-sky column SW absorption at Manus derived from the satellite/surface observations (105.5 W m^{-2}) was about 12% higher than that calculated using the radar-derived cloud properties (93.3 W m^{-2}), while the clear-sky column SW absorption was more similar (93.9 W m^{-2} for satellite/surface and 91.5 W m^{-2} for calculations). This difference, while still an underestimate of all-sky absorption for the radiative transfer calculations, is on the order of the difference seen in recent aircraft studies of overcast cloud cases [*Asano et al.*, 2000; *Ackerman et al.*, 2003; *O'Hirok and Gautier*, 2003] and is significantly less than the 30% underestimates seen in the satellite/surface comparison studies of the 1990s [*Cess et al.*, 1995]. However, the satellite/surface observations in the current study produced a range of variation in daily-averaged all-sky column absorption (38–177 W m^{-2}) that cannot be matched using realistic radar-derived cloud properties and a one-dimensional radiative transfer model. The existence of both large underestimates and overestimates of column absorption from the satellite/surface observations (Figure 10) indicates that spatial mismatch and apparent absorption due to three-dimensional effects may be a factor in such comparisons even on the daily-average timescale.

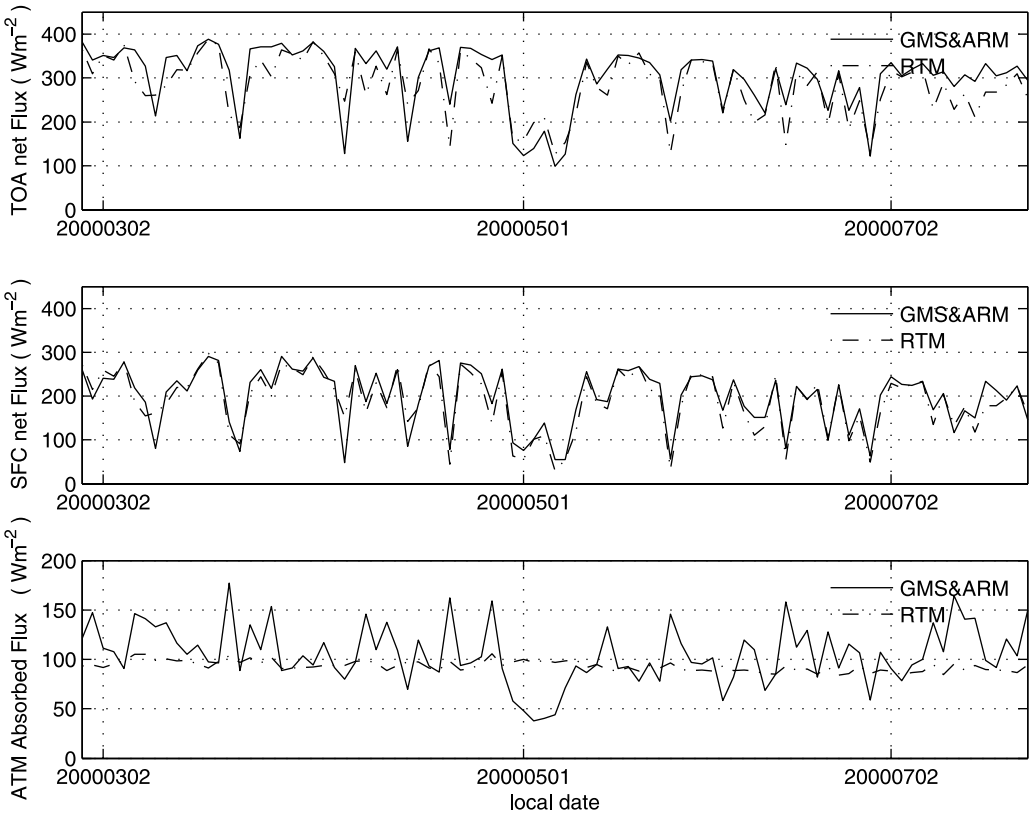

Figure 10. Daily-average all-sky SW broadband (top) net flux at TOA, (middle) net flux at surface, and (bottom) absorbed flux in column from satellite/surface observations (GMS and ARM) and from radiative transfer calculations using radar-derived cloud properties (RTM).

[55] In future work, we plan to carry out a more comprehensive column radiation closure study using surface flux data from the ARM site and TOA fluxes from geostationary satellite observations to further examine reasons for the underestimation of and much smaller range in column absorption calculated with a radiative transfer model using retrieved cloud properties compared to that calculated from the measured surface and TOA fluxes on the daily-average timescale. Several avenues to explore include the spatial, geometrical, and temporal mismatch between surface flux, satellite flux, and radar reflectivity measurements; sensitivity to cloud retrieval assumptions; three-dimensional radiative transfer effects; and the possibility of instantaneous errors in TOA fluxes from geostationary satellites due to the issues involved in converting from narrowband radiance to broadband flux [*Nordeen et al.*, 2001; *Loeb et al.*, 2007].

5. Conclusions

[56] In this study we examined the vertical redistribution of SW absorption in the tropical atmosphere due to clouds. Simple sensitivity studies illustrated that low-level tropical clouds always increase the total SW absorption in the column relative to clear sky because of cloud particle absorption and increased water vapor absorption due to SW reflection from cloud top. Mid- and high-level clouds can increase or decrease absorption (depending on vertical location, particle size, and WV column amount) because of competing effects of cloud particle absorption and reduced water vapor absorption due to reflected SW radiation.

[57] Calculations based on high-vertical resolution profiles of cloud properties retrieved from cloud radar at the Manus and Nauru sites indicate that the effects of liquid and ice clouds on the total column absorption tend to compensate over the diurnal cycle, leading to small differences in the daily-averaged column absorption for clear and cloudy columns. The average effect of clouds on the daily-averaged column absorption over the study period was less than 5 W m^{-2} at both sites, although there was a strong effect on the vertical distribution of the SW absorption. These results indicate that knowledge of the total column absorption is not sufficient to understand the vertical redistribution of SW radiation in the atmosphere by clouds and its impact on local and large-scale dynamics. Clouds concentrate the absorption of solar radiation into particular atmospheric layers, relative to the broad absorption throughout the troposphere seen in clear sky, having important impacts on both cloud-scale and large-scale dynamics. Further studies are needed to identify the vertical resolution required to capture features of the vertical cloud property and heating profiles that are important to local and large-scale dynamics.

[58] The effect of clouds on the vertical distribution of SW absorption at the two sites varied primarily because of the differing frequency of high clouds at the two sites. The variability in absorption with cloud type frequency indicates that changes in cloud properties or cloud vertical structure are likely to have differing regional impacts.

[59] Comparisons to daily-averaged column absorption values calculated by combining satellite and surface flux observations indicated that the calculations using the radar-derived cloud properties and a one-dimensional radiative transfer model underestimated the column absorption by 12% at Manus and could not match the range of variability seen in the satellite/surface observations. This underestimate of all-sky column absorption is on the same order of magnitude as recent results from aircraft studies of overcast clouds and is significantly less than previous studies with hourly surface/satellite observations. Further analysis of the uncertainties associated with deriving column absorption from satellite and shortwave observations with such different spatial and temporal scales is planned.

[60] **Acknowledgments.** The authors thank Dr. Laura Hinkelman and three anonymous reviewers for their helpful comments on the manuscript. The Pacific Northwest National Laboratory is operated by Battelle for U.S. Department of Energy (DOE). This research was supported by the DOE office of Biological and Environmental Research as part of the Atmospheric Radiation Measurement (ARM) program. The ARM surface data were obtained from the ARM archive (www.archive.arm.gov). The TOA fluxes from the GMS-5 satellite were calculated by the NASA Langley Cloud and Radiation Research Group and were also obtained from the ARM archive.

References

Ackerman, T. P., D. M. Flynn, and R. T. Marchand (2003), Quantifying the magnitude of anomalous solar absorption, *J. Geophys. Res.*, *108*(D9), 4273, doi:10.1029/2002JD002674.

Arking, A. (1996), Absorption of solar energy in the atmosphere: Discrepancy between model and observations, *Science*, *273*, 779–782.

Asano, S., A. Uchiyama, Y. Mano, M. Murakami, and Y. Takayma (2000), No evidence for solar absorption anomaly by marine water clouds through collocated aircraft radiation measurements, *J. Geophys. Res.*, *105*, 14,761–14,775.

Barker, H. W., and Z. Li (1997), Interpreting shortwave albedo-transmittance plots: True or apparent anomalous absorption?, *Geophys. Res. Lett.*, *24*, 2023–2026.

Barker, H. W., J. J. Morcrette, and G. D. Alexander (1998), Broadband solar fluxes and heating rates for atmospheres with 3d broken clouds, *Quart. J. R. Met. Soc.*, *124*, 1245–1271.

Cess, R. D., et al. (1995), Absorption of solar radiation by clouds: Observations versus models, *Science*, *267*, 496–499.

Comstock, J. M., et al. (2007), An intercomparison of microphysical retrieval algorithms for upper tropospheric ice clouds, *Bull. Amer. Meteorol. Soc.*, *88*, 191–204.

Crisp, D. (1997), Absorption of sunlight by water vapor in cloudy conditions: A partial explanation for the cloud absorption anomaly, *Geophys. Res. Lett.*, *24*, 571–574.

DiGiuseppe, F., and A. M. Tompkins (2003), Three-dimensional radiative transfer in tropical deep convective clouds, *J. Geophys. Res.*, *108*(D23), 4741, doi:10.1029/2003JD003392.

DiGiuseppe, F., and A. M. Tompkins (2005), Impact of cloud cover on solar radiative biases in deep convective regimes, *J. Atmos. Sci.*, *62*, 1989–2000.

Erlick, C., V. Ramaswamy, and L. M. Russell (2006), Differing regional responses to a perturbation in solar cloud absorption in the SKYHI general circulation model, *J. Geophys. Res.*, *111*, D06204, doi:10.1029/2005JD006491.

Fu, Q. (1996), An accurate parameterization of the solar radiative properties of cirrus clouds for climate models, *J. Clim.*, *9*, 2058–2082.

Fu, Q., and K. N. Liou (1992), On the correlated *k*-distribution method for radiative transfer in nonhomogeneous atmospheres, *J. Atmos. Sci.*, *49*, 2139–2156.

Fu, Q., M. C. Cribb, H. W. Barker, S. K. Krueger, and A. Grossman (2000), Cloud geometry effects on atmospheric solar absorption, *J. Atmos. Sci.*, *57*, 1156–1168.

Garrett, T. J., H. Gerber, D. G. Baumgardener, C. H. Twohy, and E. M. Weinstock (2003), Small, highly reflective ice crystals in low-latitude cirrus, *Geophys. Res. Lett.*, *30*(21), 2132, doi:10.1029/2003GL018153.

Inness, P. M., J. M. Slingo, S. J. Woolnough, R. B. Neale, and V. D. Pope (2001), Organization of tropical convection in a gcm with varying vertical resolution; implications for the simulation of the Madden-Julian Oscillation, *Clim. Dyn.*, *17*, 777–793.

Ivanova, D., D. L. Mitchell, W. P. Arnott, and M. Poellot (2001), A GCM parameterication for bimodal size spectra and ice mass removal rates in mid-latitude cirrus clouds, *Atmos. Res.*, *59–60*, 89–113.

Johnson, R. H., and P. E. Ciesielski (2000), Rainfall and radiative heating rates from TOGA COARE atmospheric budgets, *J. Atmos. Sci.*, *57*, 1497–1514.

Kim, D., and V. Ramanathan (2008), Solar radiation budget and radiative forcing due to aerosols and clouds, *J. Geophys. Res.*, *113*, D02203, doi:10.1029/2007JD008434.

Kubota, H., A. Numaguti, and S. Emori (2004), Numerical experiments examining the mechanism of diurnal variation of tropical convection, *J. Met. Soc. Jpn.*, *82*, 1245–1260.

Li, Z., C. H. Whitlock, and T. P. Charlock (1995), Assessment of the global monthly mean surface insulation estimated from satellite measurements using global energy-balance archive data, *J. Clim.*, *8*, 315–328.

Li, Z., M. C. Cribb, and F. L. Chang (2005), Natural variability and sampling errors in solar radiation measurements for model validation over the Atmospheric Radiation Measurements Southern Great Plains region, *J. Geophys. Res.*, *110*, D15S19, doi:10.1029/2004JD005028.

Loeb, N. G., S. Kato, K. Loukachine, N. Manalo-Smith, and D. R. Doelling (2007), Angular distribution models for top-of-atmosphere radiative flux estimation from the clouds and the earth's radiant energy system instrument on the Terra satellite: part II. Validation, *J. Atmos. Ocean. Technol.*, *24*(4), 564–584.

Long, C. N., and T. P. Ackerman (2000), Identification of clear skies from broadband pyranometer measurements and calculation of downwelling shortwave cloud effects, *J. Geophys. Res.*, *105*, 15,609–15,626.

Lubin, D., J.-P. Chen, P. Pilewskie, V. Ramanathan, and F. P. J. Valero (1996), 1996: Microphysical examination of excess cloud absorption in the tropical atmosphere, *J. Geophys. Res.*, *101*, 16,961–16,972.

Mather, J. H., T. P. Ackerman, W. E. Clements, F. J. Barnes, M. D. Ivey, L. D. Hatfield, and R. M. Reynolds (1998), An atmospheric radiation and cloud station in the Tropical Western Pacific, *Bull. Amer. Meteorol. Soc.*, *79*, 627–642.

Mather, J. H., S. A. McFarlane, M. A. Miller, and K. L. Johnson (2007), Cloud properties and associated heating rates in the tropical western Pacific, *J. Geophys. Res.*, *112*, D05201, doi:10.1029/2006JD007555.

McFarlane, S. A., and K. F. Evans (2004a), Clouds and shortwave fluxes at Nauru: part I. Retrieved cloud properties, *J. Atmos. Sci.*, *61*, 733–744.

McFarlane, S. A., and K. F. Evans (2004b), Clouds and shortwave fluxes at Nauru: part II. Shortwave flux closure, *J. Atmos. Sci.*, *61*, 2602–2615.

McFarlane, S. A., J. H. Mather, and T. P. Ackerman (2007), Analysis of tropical radiative heating profiles: A comparison of models and observations, *J. Geophys. Res.*, *112*, D14218, doi:10.1029/2006JD008290.

McFarquhar, G. M. (2001), Comments on "parameterization of effective sizes of cirrus-cloud particles and its verification against observations", *Quart. J. R. Met. Soc.*, *127*, 261–265.

McFarquhar, G. M., J. Um, M. Freer, D. Baumgardner, G. Kok, and G. G. Mace (2007), Importance of small ice crystals to cirrus properties: Observations from the Tropical Warm Pool International Cloud Experiment (TWP-ICE), *Geophys. Res. Lett.*, *34*, L13803, doi:10.1029/2007GL029865.

Nordeen, M. L., P. Minnis, D. R. Doelling, D. Pethick, and L. Nguyen (2001), Satellite observations of cloud plumes generated by Nauru, *Geophys. Res. Lett.*, *28*, 631–634.

O'Hirok, W., and C. Gautier (2003), Absorption of shortwave radiation in a cloudy atmosphere: Observed and theoretical estimates during the second atmospheric radiation measurement enhanced shortwave experiment (ARESE), *J. Geophys. Res.*, *108*(D14), 4412, doi:10.1029/2002JD002818.

Ramaswamy, V., and S. M. Freidenreich (1998), A high-spectral resolution study of the near-infrared solar flux disposition in clear and overcast atmospheres, *J. Geophys. Res.*, *103*, 23,355–23,273.

Rothman, L. S., et al. (2003), The HITRAN molecular spectroscopic database: Edition of 2000 including updates through 2001, *J. Quant. Spectrosc. Radiat. Transfer*, *82*, 5–44.

Smirnov, A., B. N. Holben, Y. J. Kaufman, O. Dubovik, T. F. Eck, I. Slutsker, C. Pietras, and R. N. Halthore (2002), Optical properties of atmospheric aerosol in maritime environments, *J. Atmos. Sci.*, *59*, 501–523.

Solomon, S., R. W. Portmann, R. W. Sanders, and J. S. Daniel (1998), Absorption of solar radiation by water vapor, oxygen, and related collision pairs in the earth's atmosphere, *J. Geophys. Res.*, *103*, 3847–3858.

Stephens, G. L. (1978), Radiation profiles in extended water clouds: part I. Theory, *J. Atmos. Sci.*, *35*, 2111–2122.

Stephens, G. L. (2005), Cloud feedbacks in the climate system: A critical review, *J. Clim.*, *18*, 237–273.

Stephens, G. L., and S.-C. Tsay (1990), On the cloud absorption anomaly, *Q. J. R. Meteorol. Soc.*, *116*, 671–704.

Sun, Z., and L. Rikus (1999), Parameterization of effective sizes of cirrus-cloud particles and its verification against observations, *Q. J. R. Meteorol. Soc.*, *125*, 3037–3055.

Vogelmann, A. M. (2002), Aerosol radiative effects in the Tropical Western Pacific, in *Proceedings of the Twelfth Atmospheric Radiation Measurement Program Science Team Meeting*, US Department of Energy, St. Petersburg, FL, 8–12 April.

Wang, J., and W. B. Rossow (1998), Effects of cloud vertical structure on atmospheric circulation in the GISS GCM, *J. Clim.*, *12*, 3010–3029.

Wang, Z., and K. Sassen (2002), Cirrus cloud microphysical property retrieval using lidar and radar measurements: part 1. Algorithm description and comparison with in situ data, *J. Appl. Meteorol.*, *41*, 218–229.

Wyser, K. (1999), Ice crystal habits and solar radiation, *Tellus*, *51A*, 937–950.

Xu, K.-M., and D. A. Randall (1995), Impact of interactive radiative transfer on the macroscopic behavior of cumulus ensembles: part II. Mechanisms for cloud-radiation interactions, *J. Atmos. Sci.*, *52*, 800–817.

T. P. Ackerman and Z. Liu, Joint Institute for the Study of the Atmosphere and Ocean and Department of Atmospheric Sciences, University of Washington, 3737 Brooklyn Ave NE, Seattle, WA 98105, USA.

J. H. Mather and S. A. McFarlane, Climate Physics Group, Pacific Northwest National Laboratory, P.O. Box 999, MS K9-24, Richland, WA 99352, USA. (sally.mcfarlane@pnl.gov)